Chaotic Modeling and Simulation (CMSIM) 1: 187-197, 2011

Using Average Mutual Information to Preview the Power Spectrum and to Guide Nonlinear Noise Reduction

N. Jevtic[a,b], W. Nilsen[a], P. Stine[a], J. S. Schweitzer[b]
[a] Bloomsburg University, 400 Second St, Bloomsburg, PA 17815, USA
[b] Physics Department, University of Connecticut, Storrs, CT 06269, USA

Abstract: Power spectra of nonlinear time series often contain relevant information across all frequencies. Traditional filtering results in loss of information at the high frequencies. Nonlinear local projective noise reduction is a method that allows us to reduce noise while retaining high-frequency information. Results for two quasi-periodic stars, a variable white dwarf and a period-doubling star, are discussed. For both, we show that average mutual information (AMI) allows us to preview the power spectrum including at higher frequencies in the white-noise tail. Once a power spectrum is obtained, AMI can also serve as an indicator of the limits to which nonlinear noise reduction can be taken.
Keywords: Nonlinear time series analysis, Power spectrum, Average mutual information, Nonlinear noise reduction, Variable stars

1 Introduction: Phase-space Portrait and the Parameters of the Time-Delay Reconstruction

One of the tools to explore nonlinear systems is a time-delay phase-space portrait. According to the embedding theorems [10, 8, 9], the geometry of this time-delay phase-space portrait is diffeomorphic to the geometry of the phase-space representation that would be obtained if the equations governing the system were known. Thus, this object is a surrogate and can be studied in lieu of the system.
To obtain a time-delay phase-space portrait of a uniformly-sampled time series, the parameters of the reconstruction have to be determined first. These are the phase-space dimension and the time delay, which are both obtained from the data.

1.1 Dimension of the Phase Space

The dimension of the reconstructed phase space is obtained using the False Nearest Neighbour (FNN) method [7] on the time series itself. This dimension is important because it is related to the number of degrees of freedom needed to model the system.

Received: 7 August 2011 / Accepted: 25 October 2011

ISSN 2241-0503

1.2 Time Delay

Autocorrelation Function

Historically the choice of the time delay was initially made using the autocorrelation function. Given N observations s_1, s_2, s_3, s_4… at times t_1, t_2, t_3, t_4,…. the autocorrelation lag τ is given by:

$$C(\tau) = \frac{1}{N-\tau} \frac{\sum_i (s_i - y)(s_{i+\tau} - y)}{\sigma^2(s)}$$

Here y is the mean and σ is the standard deviation. The autocorrelation function quantifies the similarity between observations as a function of the time separation between them. The options for the time delay are the correlation time, the zero or the minimum of the autocorrelation function.

Average Mutual Information

Over time the trend has been to choose the optimal time delay at the minimum of average mutual information [3]. Average mutual information (AMI) is an information-theory analog to the autocorrelation function. AMI is defined in terms of probabilities as:

$$AMI(\tau) = \sum_{i,j} p_{i,j} \log_2 \left[\frac{p_{i,j}}{p_i p_j} \right]$$

AMI is the amount of information (in bits) shared by the signal and its time shifted value averaged over the orbit. It is a measure of how much one learns from one signal about the other.
For a uniformly sampled time series such as a stellar light curve AMI is:

$$AMI(\tau) = \sum_{s(t),s(t+\tau)} P(s(t), s(t+\tau)) \log_2 \left[\frac{P(s(t), s(t+\tau))}{P(s(t))P(s(t+\tau))} \right]$$

Here **s** is the sampled scalar time series and τ is the time delay. The range of the time series is divided into m sub-intervals and a histogram is obtained that yields the probability p_i for a point to be in the interval i, the probability p_j for a point to be in the interval j, and the joint probability $p_{i,j}$ that if s_k is in interval i then $s_{k+\tau}$ is in interval j.
Whether the first, local minimum, or the global minimum best determine the optimal delay is still a point open to discussion.

Though AMI is analogous to the autocorrelation function of linear signal processing, it is more general in the statistical sense since the autocorrelation is the expectation of a quadratic polynomial statistic, while AMI represents the expectation of the average degree of independence incorporating all higher orders. Though AMI was initially used to obtain the optimal time delay for time-delay embeddings its probabilistic nature gives it wider applicability [2].

2 Locally-projective nonlinear noise reduction

The measured data are assumed to be the output of a low-dimensional dynamical system and random high-dimensional noise. This noise spreads the data off its manifold in phase space. For small amplitude noise, it is assumed the data are distributed closely around the manifold [4, 5].
In order to reduce noise it is therefore important to first identify this manifold and then to orthogonally project the data points onto it. For a trajectory whose delay vectors a_n lie inside a m-dimensional manifold, while the dynamical system with noise forms a q-dimensional manifold where q>m. To reduce noise we over-embed and repeat the process until, due to iteration, the average correction ceases to decrease rapidly. An example of the application of the method is detailed in Jevtic et al. [6].
However, reducing noise in signals from nonlinear systems poses unique challenges. Most nonlinear systems have broadband power spectra. Differentiating noise from signal in such spectra is difficult if not impossible. It would be to great advantage if the shape of the spectrum buried by noise were known. Moreover, in such spectra, over-reduction can result in spurious results. An indication when to stop nonlinear noise reduction would greatly reduce the generation of spurious results. We will show that average mutual information can be used to advantage in both of these cases.

3 Requirements on the data

At this time, nonlinear phase-space reconstruction can only be used for uniformly-sampled continuous data sets.

4 Data Analysis

The light-curve data for two quasi-periodic stars are analysed. For a variable white dwarf and a period-doubling star we show that average mutual information (AMI) is a better predictor of the power spectrum since it can preview what is under the noise. It can also serve as a guide to when to stop nonlinear noise reduction to guard against spurious results.
For the period-doubling star for which long continuous light curves are available, phase-space portraits and power spectra are investigated for sub-intervals over time.

DB White Dwarf PG1351+489

Eleven hours of continuous DB white dwarf PG1351+489 data were analysed [6], Fig. 1. This section of the light curve was obtained by the ground-based Whole Earth Telescope international collaboration during its xCov12 campaign.

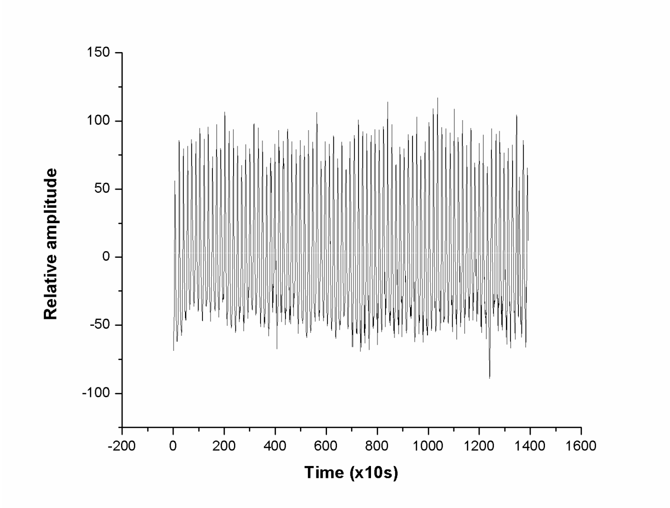

Fig. 1. PG 1351+489 light curve

The autocorrelation function (black curve) and the Average Mutual Information (AMI) (red curve) for the above data are shown in Fig. 2. The two curves are

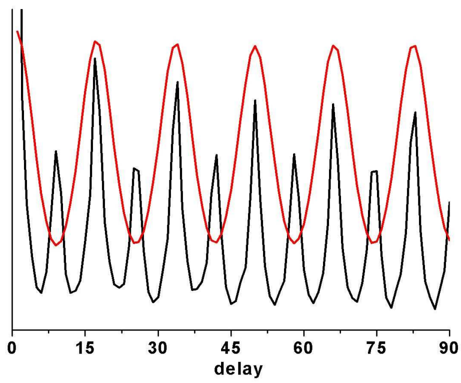

Fig. 2. PG 1351+489 autocorrelation function (gray) and Average Mutual Information (AMI) (black)

scaled to the first maximum. The correlation function (red curve) indicates the presence of only a single periodicity. The AMI (black curve) indicates a "primary" comb of a fundamental and harmonics whose magnitude diminishes with delay. A "secondary" comb of sub-harmonics is also present between the "primary" ones which has constant magnitude.

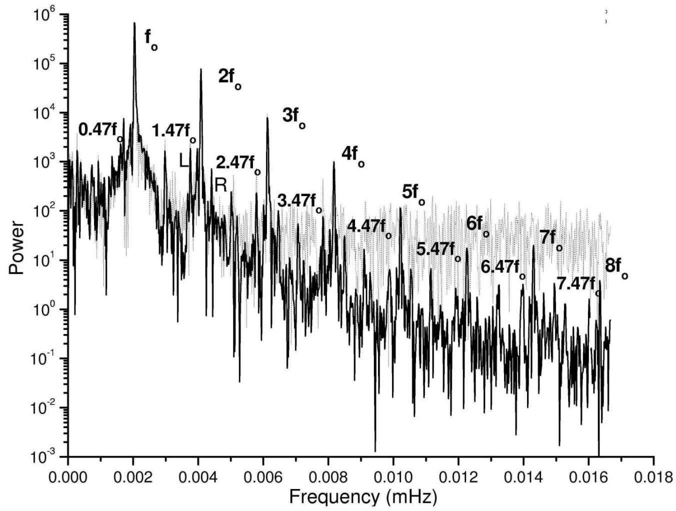

Fig. 3 PG 1351+489 power spectra before (gray) and after noise reduction (black)

Power spectra for white dwarf PG 1351+489 before (gray) and after noise reduction (black) are shown in Fig. 3 for ~11h of data. The black power spectrum is after noise reduction from 7 dimensions with 6 iterations. The white-noise tail is lowered by a factor of ~50. More lines were identified than from the whole xCov12 run of 84 h [1]. Thus noise reduction allows us to shorten the data-collection time by a factor of 7.

In both power spectra, as predicted by AMI, a fundamental and its harmonics are present. Also, there is a comb of sub-harmonics. Moreover, the line amplitude diminishes with frequency.

TYC 3544-1245-1

The second star analysed is listed in the Tycho2 catalogue as TYC 3544-1245-1. Its light curve is shown in Fig. 4.

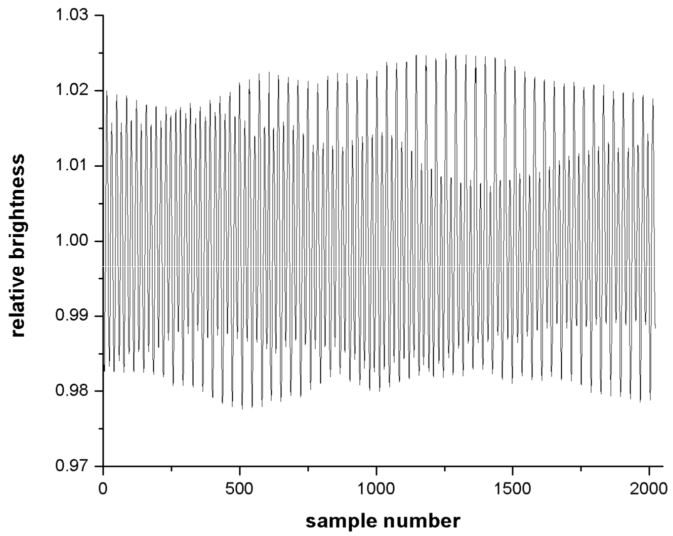

Fig 4. TYC 3544-1245-1 Light Curve

Though there is period doubling, the classification of this star is still being debated. At times it has been classified as a solar-like star, an RR Lyrea star, a delta Scuti star and a W UMa contact binary. However, for the purposes of this paper, behaviour not classification is important.

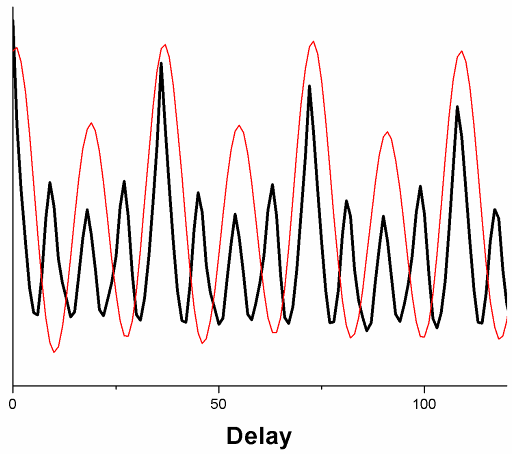

Fig. 5 Autocorrelation function (red) and Average Mutual Information (AMI) (black) for TYC 3544-1245-1

In Fig. 5 the correlation function (red curve) indicates the presence of a periodicity and its harmonics and a single sub-harmonic all of constant amplitude. The AMI (black) curve also indicates that the periodicities present consist of a “primary” comb consisting of a fundamental frequency and its harmonics but the single sub-harmonic has become a “secondary” comb of three smaller sub-harmonics between subsequent “primary” peaks. The amplitudes of the “primary” comb diminish with delay while the amplitudes of the “secondary” comb remain constant.

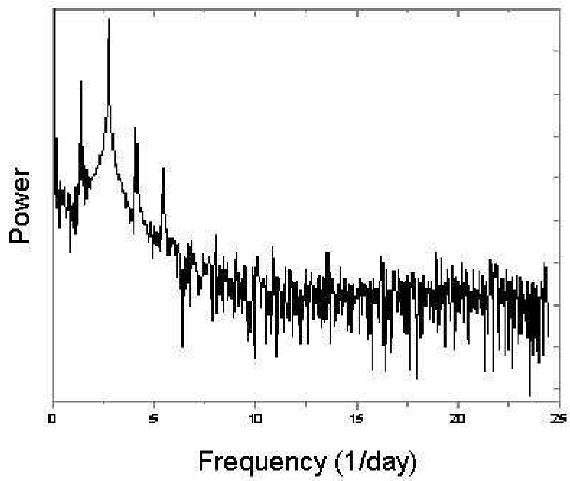

Fig. 6 The power spectrum of three months of data for TYC 3544-1245-1

The power spectrum of three months of TYC 3544-1245-1 data is shown in Fig. 6. This spectrum has a significant noise contribution and widened line bases. It does not agree with the “prediction” of the AMI.

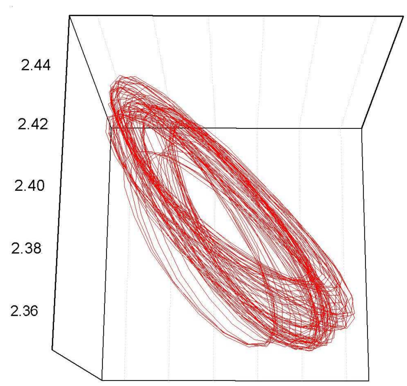

Fig. 7. TYC 3544-1245-1 phase-space portrait with evident changes in the dynamics

However, the phase-space portrait for the same period (Fig. 7) indicates that behaviour changed over time. As a result the data were divided into one month intervals and the last month was further subdivided into two fifteen-day segments. The results of nonlinear projective local noise reduction for the two last month two fifteen-day segments are shown in Fig. 8.

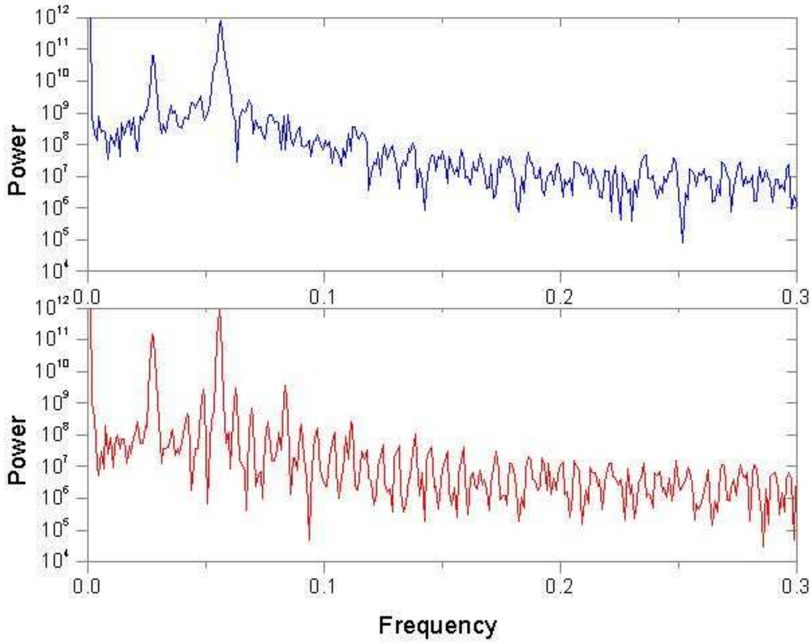

Fig. 8 Comparison of the power spectra for the two consecutive 15-day intervals after noise reduction: blue - 1st interval (top); red - 2nd interval (bottom).

The power spectra after nonlinear noise reduction for the two fifteen-day intervals are compared in Fig. 8. Noise reduction was considerably more efficient for the second. For the 2nd fifteen-day interval the AMI prediction of a comb of primary frequencies of diminishing amplitude with delay, and a triplet of smaller sub-harmonics between primary peaks can be seen to be correct. However, the number of "primary" harmonics that can be identified has not increased.

Since the red power spectrum for the second 15 days can be interpreted as a change in the dynamics, the search for an explanation led to a second inspection of the phase-space portraits of the two 15-day intervals separately.

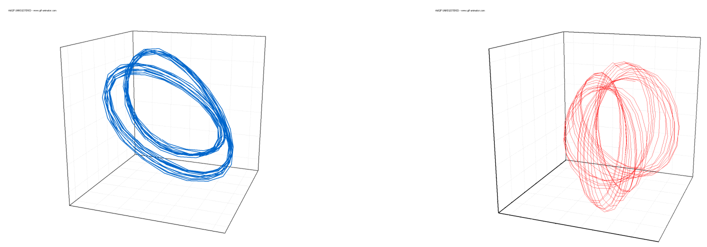

Fig. 9 Phase-space portraits of the two 15-day intervals (figures are color-coded to correspond to the top and bottom power spectrum in Fig. 8, respectively.).

Noise reduction was much more efficient for the second (red) segment that has a more developed surface in phase space due to de-threading. Thus we observe all the frequencies predicted by AMI due to an interplay of a moderate parameter change and the nature of that change that allows for efficient noise reduction.
A second noise reduction resulted in the power spectra shown in Fig. 10.

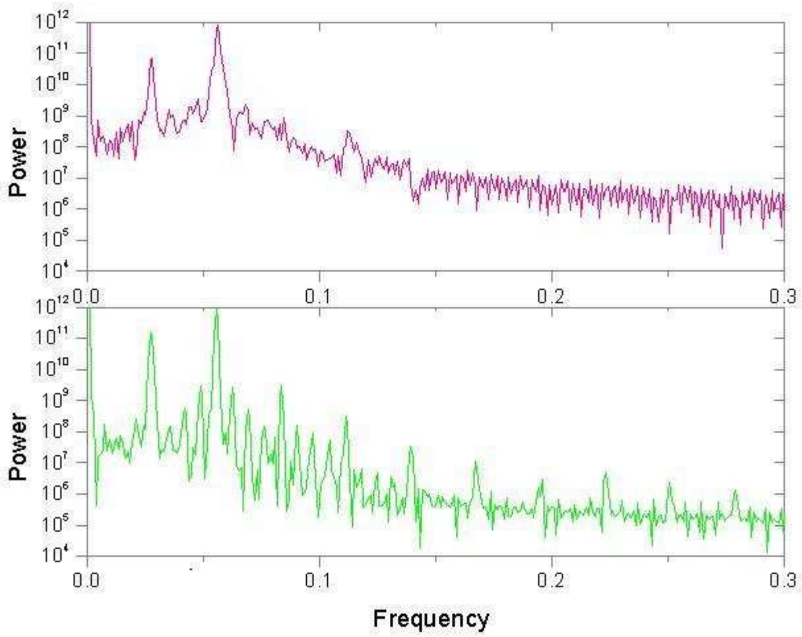

Fig. 10 Power spectra of the two 15-day intervals after a second round of nonlinear noise reduction: 1st interval (top-violet); 2nd interval (bottom-green).

The power spectra of the two 15-day data sets after a second round of nonlinear noise reduction in Fig. 10 are an illustration of another aspect of the utility of AMI.

For the second interval power spectrum (rendered in green), the number of accessible “primary” harmonics has increased dramatically. However, the “triplet sub-comb” predicted by AMI has been considerably suppressed at the higher frequencies. If the bottom (2^{nd} interval-green) spectrum is compared with the top (1^{st} interval-violet) 15-day power spectrum in Fig. 10, at the higher frequencies the onset of the region in which the triplets are over-suppressed in the bottom (green) spectrum corresponds to the onset of spurious structures in the top (violet) spectrum. Thus, AMI can also be used to estimate when noise reduction should be stopped to avoid the introduction of artefacts. In practice, fewer iterations will protect against this.

5 Conclusions

Average Mutual Information (AMI) remains the most effective tool to select the optimal delay for time-delay phase space reconstruction. Earlier work [2] demonstrated the predictive value of a variant of average mutual information in the time domain. In the frequency domain, for quasi-periodic light curves, we show that AMI is a much more powerful tool than generally appreciated. For the light curves considered, AMI over a range of delays previews the shape of the Fourier power spectrum with fidelity even when there is considerable white noise present.

Moreover, as complexity grows with the increase of the number of sub-harmonics present the autocorrelation function, the AMI linear analog, continually underestimates the multiplicity of sub-harmonics. Even without a definitive, more extensive study of a variety of light-curve shapes, it is safe to say, by analogy, that AMI yields a reliable estimate for the lower bound on the multiplicity of sub-harmonics.

A preview of the power spectrum is a major advantage when reducing noise in signals from nonlinear systems which have broadband power spectra. Differentiating noise from signal in such spectra is difficult if not impossible. However, there is an additional benefit in that AMI also allows us to set limits on when noise reduction should be stopped since over-reduction may lead to spurious results. Knowing when noise reduction starts suppressing parts of the power spectrum that are actually integral to it and needed to model the dynamics is also extremely valuable.

Of the two light curves used to illustrate this new approach to AMI, the TYC 3544-1245-1 data proved to be the more interesting. Period doubling was detected for TYC 3544-1245-1. In addition, the phase-space portrait for two successive intervals indicated a moderate change in dynamics that resulted in de-threading [6] leading to a surface that allows for more efficient noise reduction. Nonlinear noise reduction for that part of the light curve resulted in a power spectrum predicted by the AMI consisting of a “primary” fundamental, its harmonics and a “secondary” sub-harmonic triplet structure between them. Moreover, even though repeated noise reduction resulted in better access to the “primary” harmonics, it proved excessive at higher frequencies suppressing the "secondary" triplet structure. This can practically be easily remedied by using a smaller number of iterations.

To our knowledge, no other method gives as good a preview of the power spectrum in the presence of considerable noise. Also, though not quantitative as yet, AMI promises to develop into a useful tool to delineate useful from artefact-generating noise reduction.

References

1. V.M. Alves et al., The Pulsating DB White Dwarf PG 1351+489, 2003, Baltic Astron., 12, 33
2. J. Chen, et al., Spatiotemporal dynamics of the magnetosphere during geospace storms: Mutual information analysis Geophys Res, VOL. 113, A05217
3. A.M. Fraser, H.L. Swinney, Independent coordinates for strange attractors from mutual information, Phys.Rev. A, 33, 2, 1986, pp.1134-1140
4. P. Grassberger, , et al., On noise reduction methods for chaotic data, CHAOS 3, 127 (1993)
5. R. Hegger, H. Kantz, and T. Schreiber, Practical implementation of nonlinear time series methods: The TISEAN package, CHAOS, 9, 413 (1999)
6. N. Jevtic et al., Nonlinear Time Series Analysis of PG1351+489 Light Intensity Curves ApJ, 635:527-539, 2005
7. M. B. Kennel et al., Determining embedding dimension for phase-space reconstruction using a geometrical construction, Phys.Rev. A 45, 3403 (1992)
8. J. Stark, Delay Embeddings for Forced Systems I: Deterministic Forcing, Journal of Nonlinear Science, 9, 255-332, 1999
9. J. Stark et al. Delay Embeddings for Forced Systems II: Stochastic Forcing, Journal of Nonlinear Science, 13, 519, 2003.
10. Takens-Mane, Detecting Strange Attractors in Turbulence, Dynamical Systems and Turbulence, 898, Lecture Notes in Mathematics (Springer-Verlag, 1981)

Acknowledgements

The WET for the PG1351+489 data: the xCov12 campaign team, particularly Antonio Kanaan and Steve Kawaler.

For the publically available data, we thank the entire Kepler team for the development and operations of this outstanding mission and all involved in KASC for the handling of the data. Their efforts have allowed us to conduct the theoretical work on nonlinear time series methodology presented herein. Funding for the Kepler Mission is provided by NASA's Science Mission Directorate.

The Bloomsburg University Faculty Travel Fund and the Bloomsburg University Foundation.

The Max Planck Institute for Complex Systems for the TISEAN software: R. Hegger, H. Kantz, and T. Schreiber, Practical implementation of nonlinear time series methods: The TISEAN package, CHAOS, 9, 413 (1999).